NEW DIFFRACTION DATA

Crystal structure of 5-(3-methoxyphenyl)indoline-2,3-dione

Anastasia Gorodnova [ORCID],[a)] Vladimir N. Ivanov, Alexander V. Kurkin, and Artem Dmitrienko [ORCID]
Lomonosov Moscow State University, Moscow, Russian Federation

The crystal structure of 5-(3-methoxyphenyl)indoline-2,3-dione ($C_{15}H_{11}NO_3$) was solved and refined using laboratory powder diffraction data and optimized using density functional techniques. The title compound crystallizes in space group *Pbca* with $a = 11.1772(3)$ Å, $b = 7.92536(13)$ Å, $c = 27.0121(7)$ Å, and $V = 2392.82(10)$ Å^3. The asymmetric unit contains one molecule. Isatin molecules are joined into almost flat chains along the *a* direction by N–H···O bonds. The chains are linked into layers by π-stacking interactions. Finally, the third dimension of the crystal is formed by weaker C–H···π and C–H···O contacts.

I. INTRODUCTION

5-(3-methoxyphenyl)isatin is a red solid material. Isatin (indole-2,3-dione, $C_8H_5NO_2$) has been known from ancient times as a pigment in the dye industry. Isatin and 6-bromoisatin were intermediates in the production of indigo and Tyrian purple and probably were minor pigments in these dyes (Ferreira et al., 2004). Isatin is widely used as a substrate for organic synthesis (da Silva et al., 2001). Recently, isatin and its derivatives have received more attention due to its diverse biological activity (Medvedev et al., 2007), including anticancer properties (Cane et al., 2000; Vine et al., 2007). Some aromatic ring-substituted derivatives of isatin are reported to exhibit cytotoxicity on a human monocyte-like histiocytic lymphoma (U937) cell line (Vine et al., 2007). Aryl-substituted isatins are promising inhibitors of matrix metalloproteinases, which are known to affect tumor progression. A two-dimensional (2D) molecular diagram for 5-(3-methoxyphenyl)isatin ($C_{15}H_{11}NO_3$) is shown in Figure 1.

II. EXPERIMENTAL

A. Synthesis

5-Iodoisatin (253 mg, 1.00 mmol) was suspended in a mixture of ethanol (10 ml) and water (10 ml) under constant flow of nitrogen. K_2CO_3 (0.41 g, 3.00 mmol, 3 equiv) was added and the mixture was heated at reflux until the solution became almost colorless (5–10 min). The solution was cooled to ambient temperature and the 3-methoxyphenylboronic acid (1.30 mmol, 1.3 equiv) was added, followed by the addition of [1,1′-Bis(diphenylphosphino)ferrocene]dichloropalladium(II) (7.30 mg, 0.10 mol. %). The reaction mixture was heated at reflux for 8 h, cooled to ambient temperature and acetic acid (10 ml) was added. The resulting mixture was heated at reflux for 10 min. If precipitate formation was seen after cooling, then it was filtered and recrystallized one more time from a hot solution of acetic acid, filtered and the catalyst residue removed. In all the other cases, the acetic acid was diluted with water (∼20 ml) and the product was extracted with ethyl acetate (3 × 10 ml). The combined organic layers were dried over Na_2SO_4, filtered and evaporated. The residue was purified via chromatography (eluent hexanes/EtOAc, 1:1, 0:1). The product was further recrystallized from ethanol. Yield: 48%, M = 121 mg. Red solid, m.p. 210–212 °C. For more general discussion about synthetic pathways towards 5-aryl-1H-isatins, see recent work (Ivanov et al., 2022).

B. Powder X-ray diffraction

The powder pattern was measured in variable slit mode on a MiniFLEX 600 powder diffractometer (Rigaku Corp., Tokyo, Japan) equipped with a Cu K$\alpha_{1,2}$ ($\lambda = 1.5418$ Å) X-ray tube, a 1D D/teX position-sensitive detector, and
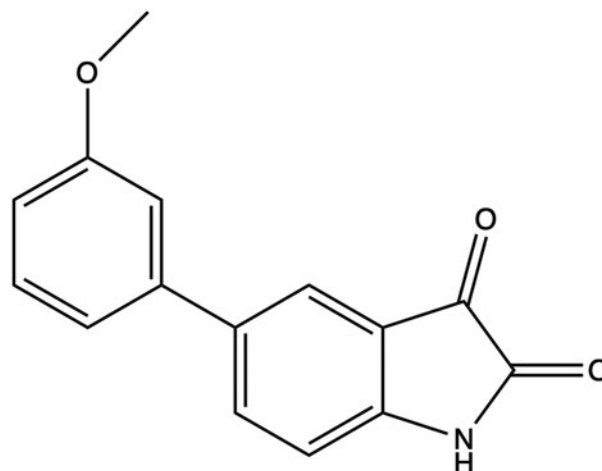

[a)]Author to whom correspondence should be addressed. Electronic mail: agorodnova6@gmail.com

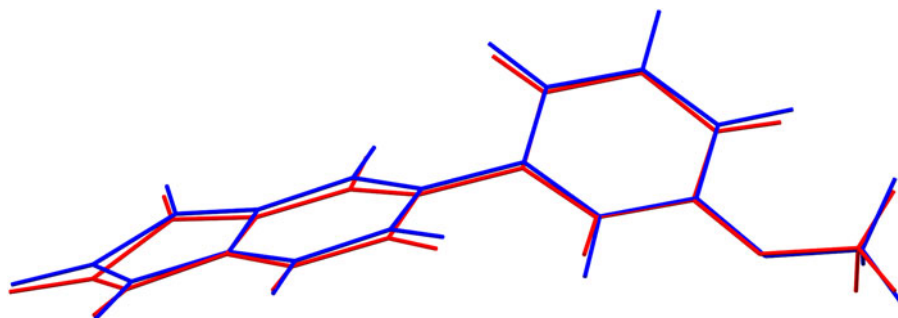Figure 1. The molecular structure of 5-(3-methoxyphenyl)isatin.

Figure 2. Comparison of the Rietveld-refined (red) and energy-optimized (blue) structures of 5-(3-methoxyphenyl)isatin.

variable divergence slits. The goniometer radius was 150 mm. Data were collected at room temperature in the range 3–90° 2θ with a 0.01° 2θ step. Since the diffractometer does not enable to measure pattern within whole range of 2θ in fixed slit mode, the powder pattern was measured in variable slit mode. The obtained pattern was then rescaled as if it had been measured in fixed slit mode with 1° divergence slit.

The pattern was indexed on a primitive orthorhombic unit cell with $a = 11.1772(3)$, $b = 7.92536(13)$, $c = 27.0121(7)$ Å, $V = 2392.82(10)$ Å^3, and $Z = 8$ by SVD-index (Coelho, 2003) as implemented in Bruker TOPAS 5.0 (Coelho, 2018). The space group suggestions were generated with ExtSym (Markvardsen et al., 2008); space group *Pbca* was chosen and confirmed by the successful structure solution and refinement. Parallel tempering, as implemented in FOX (Favre-Nicolin and Černý, 2002), was used to solve the crystal structure in direct space. The Rietveld refinement (with Bruker TOPAS 5.0) was carried out using bond and angle restraints, based on a structure of the similar isatin derivative. Restraint weight was automatically decreased during the refinement, and refinement result of more restrained model served as a starting structure for the next less restrained one.

C. DFT calculations

PW-DFT-D calculations carried out in Quantum Espresso 7.1 (Giannozzi et al., 2009, 2017) using the PBE functional (Perdew et al., 1996), Grimme D3 van der Waals correction (Grimme et al., 2010) with Becke-Johnson damping (Grimme et al., 2011), and a plane-wave basis set with projector augmented wave (PAW) pseudopotentials (Blöchl, 1994; Kresse and Joubert, 1999) from PSLibrary (Corso, 2014). Constant cell optimization was performed with the recommended cutoff of 640 eV; for variable cell optimization, the cutoff was increased by a factor of 1.3. Default 0.5 Å^{-1} k-point mesh and 2 k-points were used in all calculations. Root-mean-square (RMS) Cartesian displacement between the Rietveld refined structure and the PW-DFT-D optimized one was calculated as suggested by Neumann (van de Streek and Neumann, 2014). Pairwise intermolecular interaction energies were estimated using CE-B3LYP approximation (Mackenzie et al., 2017) in CrystalExplorer (Spackman et al., 2021).

III. RESULTS AND DISCUSSION

The pattern calculated from the initial structure obtained from FOX showed poor agreement with the experimental pattern, until preferred orientation was taken into account. Platy morphology with {001} as the major faces was suggested by the BFDH (Donnay and Harker, 1937) method in Mercury (Macrae et al., 2008). The March coefficient was close to 0.9. As only 30 mg of the title compound was available, we were not able to prepare less textured sample. The texture was added to the FOX model, and the direct-space search was repeated; the difference between the initial
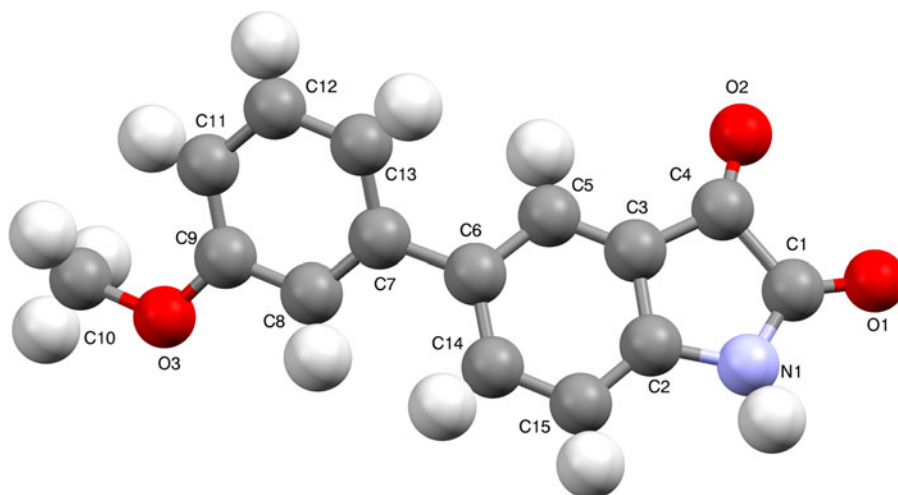

Figure 3. The asymmetric unit of 5-(3-methoxyphenyl)isatin, with the atom numbering. The atoms are represented by 50% probability spheroids.
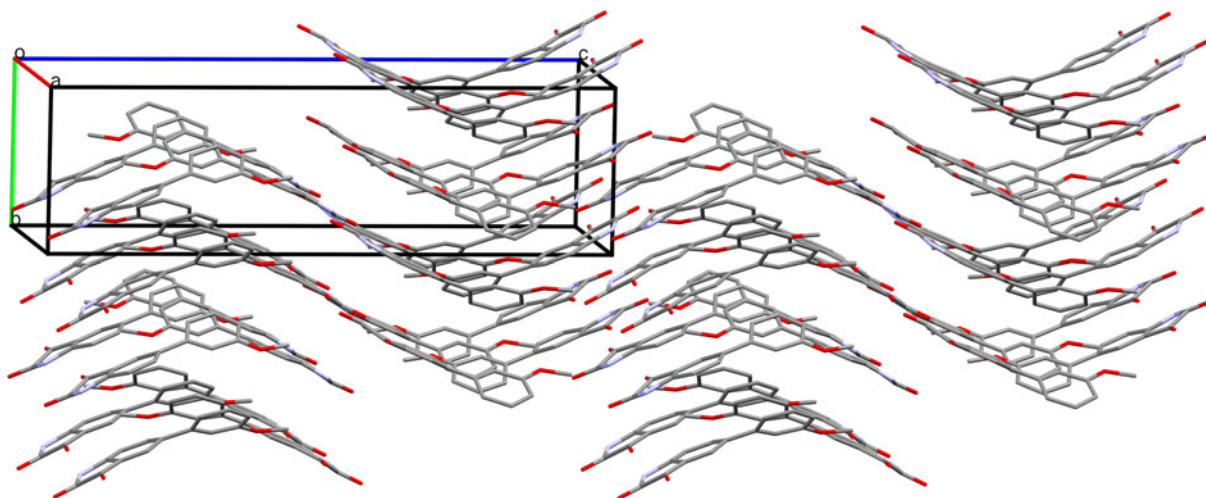
Figure 4. Fragment of the crystal packing of 5-(3-methoxyphenyl)isatin.

structure and the new one was minor. We used the new structure as a starting model for DFT optimization and Rietveld refinement.

We used a closely related structure of 5-(4-hexylphenyl) isatin (CSD Ref. code EWUVAU) (Porada et al., 2011) as a source of bond and angle restraints for the Rietveld refinement. We did not use DFT-optimized values to keep refinement and validation procedures separate. We also abandoned the idea of using mean values from Mogul check as restraints. *N*-unsubstituted isatins have a peculiar bond length alternation comparing to other indole derivatives (with an elongated C7–C8 bond as the main difference).

Although there are 40 of them in the CSD, Mogul finds more than 3000 of (not so) similar compounds. As a result, even accurate isatin structures determined from single crystal experiments have unusual bonds and angles according to the Mogul check with default parameters.

Final refinement yielded $R_p/R_p'/R_{wp}/R_{wp}' = 1.86/4.85/2.34/5.37\%$, GOF = 2.29. The March coefficient for the final structure is 0.87. The RMS Cartesian displacement of non-hydrogen atoms between free-cell energy-optimized structure and final Rietveld refined structure is 0.311 Å, which is higher than expected for a high-quality powder structure but has not surpassed the upper RMS limit for a corect structure
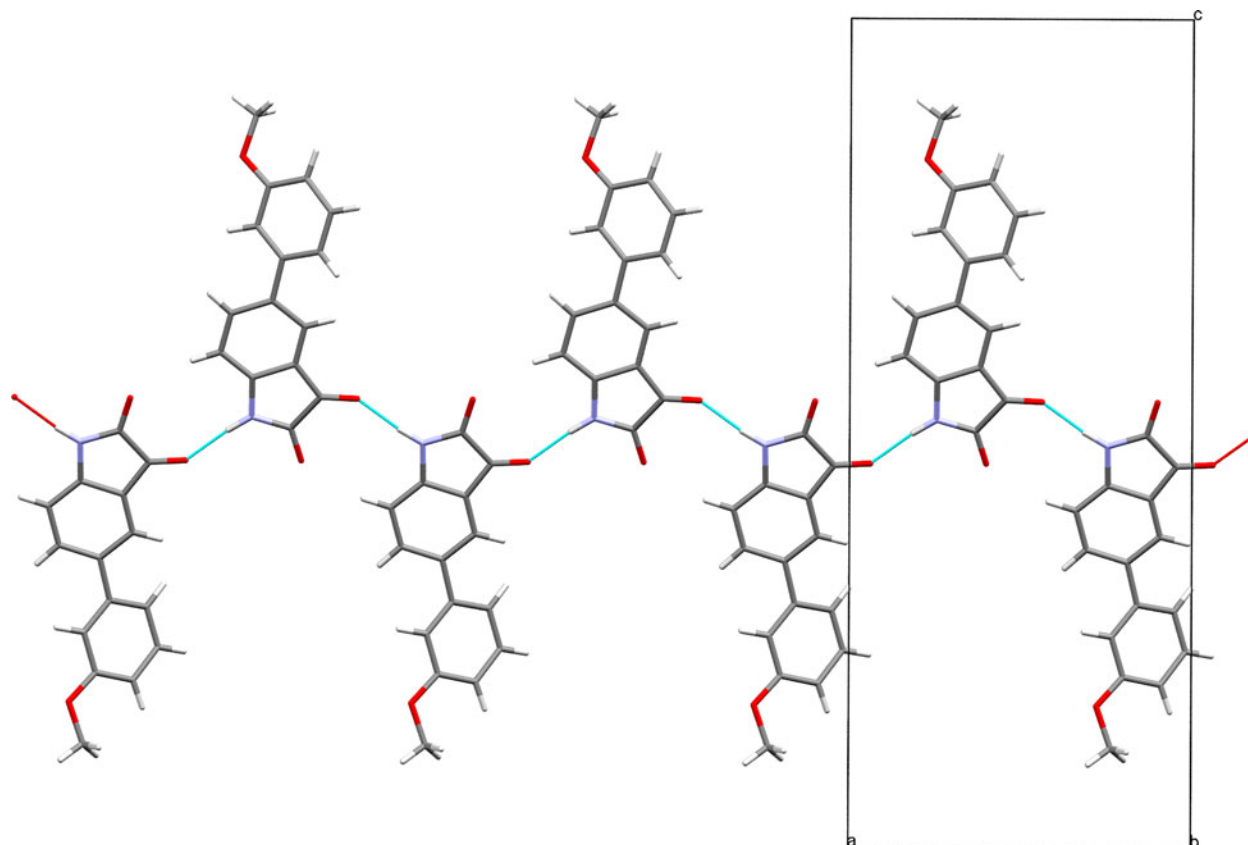

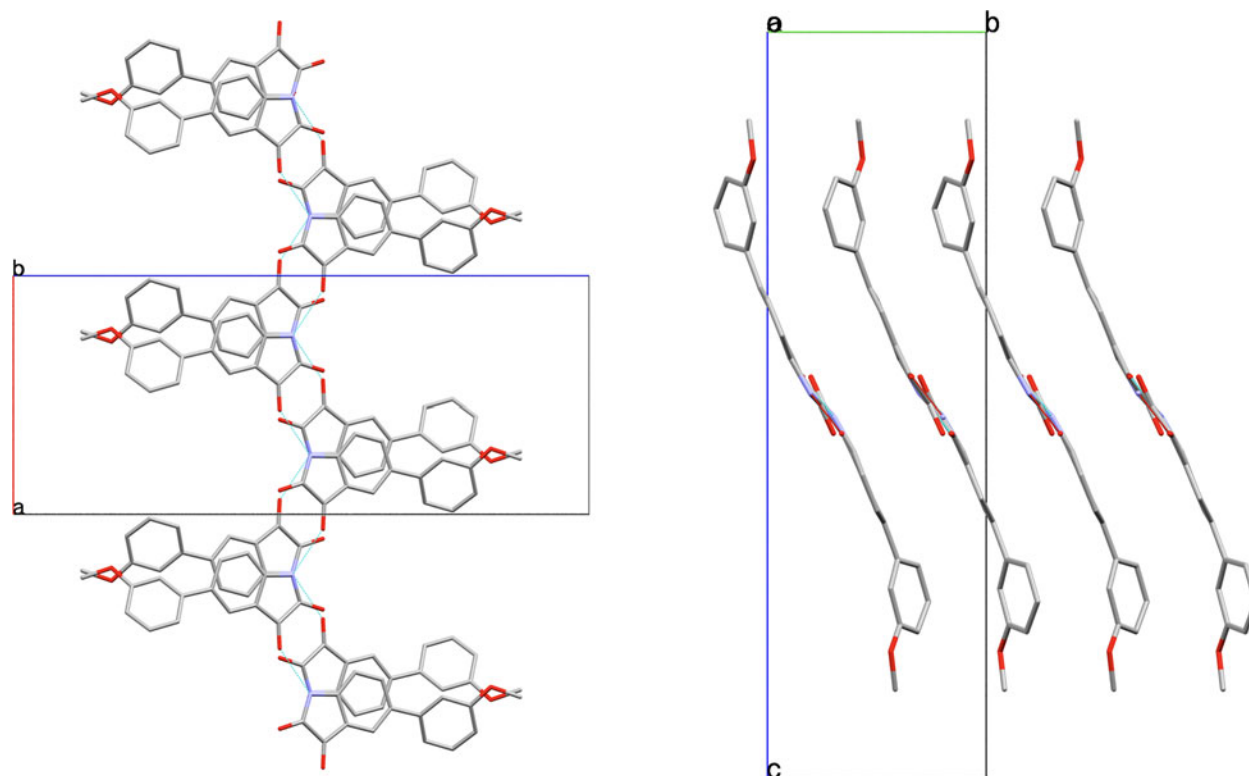Figure 5. The principal classical hydrogen bonds of 5-(3-methoxyphenyl)isatin.

Figure 6. The bilayers of 5-(3-methoxyphenyl)isatin chains, connected with C–H⋯π and C–H⋯O contacts.

(van de Streek and Neumann, 2014). We believe that the main source of the error is preferred orientation. Comparison of the final Rietveld refined structure with variable cell energy-minimized structure is shown in Figure 2.

Mogul check (2020 version, with default parameters) indicates that the C2–N1 and C2–C3 bond distances in the structure of 5-(3-methoxyphenyl)isatin are unusual, with Z-scores of 4.8 and 4.6. The deviation from Mogul's mean values was not unexpected as corresponding bond distances of the significant number of N-unsubstituted isatins are also marked as unusual.

Platon/checkCIF yields an alert on the long (1.58 Å) C1 ($sp2$)–C4($sp2$) bond. The elongation of this bond compared with mean values is also intrinsic for N-unsubstituted isatin derivatives.

Figure 3 depicts the asymmetric unit (with atom numbering) and the packing of 5-(3-methoxyphenyl)isatin is presented in Figure 4.

The isatin molecule contains one classical hydrogen bond donor (N1–H4) and two hydrogen bond acceptors (O1, O2). Therefore, the structure motifs of isatin derivatives are diverse, compared to other small rigid molecules. It forms H-bonded
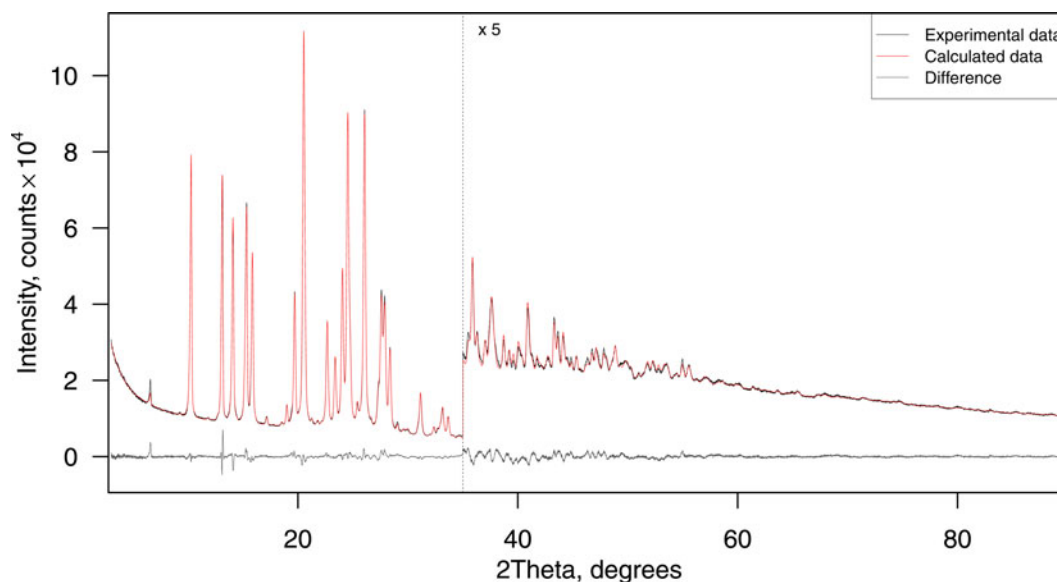

Figure 7. Final observed (black), calculated (red), and difference profiles for the Rietveld refinement.

centrosymmetric dimers (Golen and Manke, 2016), two types of chains (N1–H⋯O1 (Wei et al., 2010) and N1–H⋯O2 (Manley-King et al., 2011)) and cyclic tetramers with $Z' = 2$ (Mohamed et al., 2008).

The structure of title compound contains H-bonded N1–H⋯O2 (Figure 5) chains along the *a* direction. The chain is almost flat and additionally stabilized by a weak hydrogen bond C15–H8⋯O1. Corresponding pairwise interaction energy is 36 kJ/mol. The chains are arranged into layers by π-stacking; the corresponding pairwise energy is even higher –44 kJ/mol. The layers are connected with weaker C–H⋯π and C–H⋯O contacts (Figure 6).

The Rietveld plot is included in Figure 7. Observed diffraction patterns are in good agreement with the calculated pattern. The largest errors in the fit are in the positions of some of the low-angle peaks and probably represent the changes in the specimen during the measurement.

IV. DEPOSITED DATA

The Crystallographic Information File containing the results of the Rietveld refinement and the raw powder diffraction pattern was deposited with ICDD and can be requested at pdj@icdd.com. The crystal structure is also available from CCDC 2223458.

REFERENCES

Blöchl, P. E. 1994. "Projector Augmented-Wave Method." *Physical Review B* 50 (24): 17953–79. doi:10.1103/physrevb.50.17953.

Cane, A., M.-C. Tournaire, D. Barritault, and M. Crumeyrolle-Arias. 2000. "The Endogenous Oxindoles 5-Hydroxyoxindole and Isatin Are Antiproliferative and Proapoptotic." *Biochemical and Biophysical Research Communications* 276 (1): 379–84. doi:10.1006/bbrc.2000.3477.

Coelho, A. A. 2003. "Indexing of Powder Diffraction Patterns by Iterative Use of Singular Value Decomposition." *Journal of Applied Crystallography* 36 (1): 86–95. doi:10.1107/s0021889802019878.

Coelho, A. A. 2018. "Topas and Topas-Academic: An Optimization Program Integrating Computer Algebra and Crystallographic Objects Written in C++." *Journal of Applied Crystallography* 51 (1): 210–18. doi:10.1107/s1600576718000183.

Corso, A. D. 2014. "Pseudopotentials Periodic Table: From H to Pu." *Computational Materials Science* 95: 337–50. doi:10.1016/j.commatsci.2014.07.043.

da Silva, J. F. M., S. J. Garden, and A. C. Pinto. 2001. "The Chemistry of Isatins: A Review from 1975 to 1999." *Journal of the Brazilian Chemical Society* 12 (3): 273–324. doi:10.1590/s0103-50532001000300002.

Donnay, J. D. H., and D. Harker. 1937. "A New Law of Crystal Morphology Extending the Law of Bravais." *American Mineralogist* 22 (5): 446–67.

Favre-Nicolin, V., and R. Černý. 2002. "FOX, Free Objects for Crystallography: A Modular Approach To Ab Initio Structure Determination from Powder Diffraction." *Journal of Applied Crystallography* 35 (6): 734–43. doi:10.1107/s0021889802015236.

Ferreira, E. S. B., A. N. Hulme, H. McNab, and A. Quye. 2004. "The Natural Constituents of Historical Textile Dyes." *Chemical Society Reviews* 33 (6): 329–36. doi:10.1039/B305697J.

Giannozzi, P., S. Baroni, N. Bonini, M. Calandra, R. Car, C. Cavazzoni, D. Ceresoli, G. L. Chiarotti, M. Cocciconi, I. Dabo, A. D. Corso, S. de Gironcoli, S. Fabris, G. Fratesi, R. Gebauer, U. Gerstmann, C. Gougoussis, A. Kokalj, M. Lazzeri, L. Martin-Samos, N. Marzari, F. Mauri, R. Mazzarello, S. Paolini, A. Pasquarello, L. Paulatto, C. Sbraccia, S. Scandolo, G. Sclauzero, A. P. Seitsonen, A. Smogunov, P. Umari, and R. M. Wentzcovitch. 2009. "QUANTUM ESPRESSO: A Modular and Open-Source Software Project for Quantum Simulations of Materials." *Journal of Physics: Condensed Matter* 21 (39): 395502. doi:10.1088/0953-8984/21/39/395502.

Giannozzi, P., O. Andreussi, T. Brumme, O. Bunau, M. Buongiorno Nardelli, M. Calandra, R. Car, C. Cavazzoni, D. Ceresoli, M. Cocciconi, N. Colonna, I. Carnimeo, A. Dal Corso, S. de Gironcoli, P. Delugas, R. A. DiStasio Jr., A. Ferretti, A. Floris, G. Fratesi, G. Fugallo, R. Gebauer, U. Gerstmann, F. Giustino, T. Gorni, J. Jia, M. Kawamura, H.-Y. Ko, A. Kokalj, E. Küçükbenli, M. Lazzeri, M. Marsili, N. Marzari, F. Mauri, N. L. Nguyen, H.-V. Nguyen, A. Otero-de-la-Roza, L. Paulatto, S. Poncé, D. Rocca, R. Sabatini, B. Santra, M. Schlipf, A. P. Seitsonen, A. Smogunov, I. Timrov, T. Thonhauser, P. Umari, N. Vast, X. Wu, and S. Baroni. 2017. "Advanced capabilities for materials modelling with quantum ESPRESSO." *Journal of Physics: Condensed Matter* 29 (46): 465901. doi:10.1088/1361-648X/aa8f79.

Golen, J. A., and D. R. Manke. 2016. "4,7-Dichloro-1*H*-indole-2,3-dione." *IUCrdata* 1 (9). doi:10.1107/s2414314616014851.

Grimme, S., J. Antony, S. Ehrlich, and H. Krieg. 2010. "A Consistent and Accurate Ab Initio Parametrization of Density Functional Dispersion Correction (DFT-D) for the 94 Elements H-Pu." *Journal of Chemical Physics* 132 (15): 154104. doi:10.1063/1.3382344.

Grimme, S., S. Ehrlich, and L. Goerigk. 2011. "Effect of the Damping Function in Dispersion Corrected Density Functional Theory." *Journal of Computational Chemistry* 32 (7): 1456–65. doi:10.1002/jcc.21759.

Ivanov, V. N., M. Agamennone, I. R. Iusupov, A. Laghezza, A. M. Novoselov, E. V. Manasova, A. Altieri, P. Tortorella, A. A. Shtil, and A. V. Kurkin. 2022. "Het(Aryl)Isatin to Het(Aryl)Aminoindoline Scaffold Hopping: A Route to Selective Inhibitors of Matrix Metalloproteinases." *Arabian Journal of Chemistry* 15 (1): 103492. doi:10.1016/j.arabjc.2021.103492.

Kresse, G., and D. Joubert. 1999. "From Ultrasoft Pseudopotentials to the Projector Augmented-Wave Method." *Physical Review B* 59 (3): 1758–75. doi:10.1103/physrevb.59.1758.

Mackenzie, C. F., P. R. Spackman, D. Jayatilaka, and M. A. Spackman. 2017. "Crystalexplorer Model Energies and Energy Frameworks: Extension to Metal Coordination Compounds, Organic Salts, Solvates and Open-Shell Systems." *IUCrJ* 4 (5): 575–87. doi:10.1107/S205225251700848X.

Macrae, C. F., I. J. Bruno, J. A. Chisholm, P. R. Edgington, P. McCabe, E. Pidcock, L. Rodriguez-Monge, R. Taylor, J. van de Streek, and P. A. Wood. 2008. "Mercury CSD 2.0 New Features for the Visualization and Investigation of Crystal Structures." *Journal of Applied Crystallography* 41 (2): 466–70. doi:10.1107/s0021889807067908.

Manley-King, C. I., J. J. Bergh, and J. P. Petzer. 2011. "Inhibition of Monoamine Oxidase by Selected C5- and C6-Substituted Isatin Analogues." *Bioorganic & Medicinal Chemistry* 19 (1): 261–74. doi:10.1016/j.bmc.2010.11.028.

Markvardsen, A. J., K. Shankland, W. I. F. David, J. C. Johnston, R. M. Ibberson, M. Tucker, H. Nowell, and T. Griffin. 2008. "Extsym: A Program to Aid Space-Group Determination from Powder Diffraction Data." *Journal of Applied Crystallography* 41 (6): 1177–81. doi:10.1107/s0021889808031087.

Medvedev, A., O. Buneeva, and V. Glover. 2007. "Biological Targets for Isatin and Its Analogues: Implications for Therapy." *Biologics: Targets and Therapy* 1 (2): 151–62. doi:btt-1-151. [pii].

Mohamed, S., S. A. Barnett, D. A. Tocher, S. L. Price, K. Shankland, and C. K. Leech. 2008. "Discovery of Three Polymorphs of 7-Fluoroisatin Reveals Challenges in Using Computational Crystal Structure Prediction as a Complement to Experimental Screening." *CrystEngComm*. doi:10.1039/b714566g.

Perdew, J. P., K. Burke, and M. Ernzerhof. 1996. "Generalized Gradient Approximation Made Simple." *Physical Review Letters* 77 (18): 3865–68. doi:10.1103/physrevlett.77.3865.

Porada, J. H., J. Neudörfl, and D. Blunk. 2011. "Synthesis and Supramolecular Organization of 5-(4-Alkylphenyl)Isatin." *Crystal Growth & Design* 11 (8): 3648–52. doi:10.1021/cg200700r.

Spackman, P. R., M. J. Turner, J. J. McKinnon, S. K. Wolff, D. J. Grimwood, D. Jayatilaka, and M. A. Spackman. 2021. "Crystalexplorer: A Program for Hirshfeld Surface Analysis, Visualization and Quantitative Analysis of Molecular Crystals." *Journal of Applied Crystallography* 54 (3). doi:10.1107/S1600576721002910.

van de Streek, J., and M. A. Neumann. 2014. "Validation of Molecular Crystal Structures from Powder Diffraction Data with Dispersion-Corrected Density Functional Theory (DFT-D)." *Acta Crystallographica Section B Structural Science, Crystal Engineering and Materials* 70 (6): 1020–32. doi:10.1107/s2052520614022902.

Vine, K. L., J. M. Locke, M. Ranson, S. G. Pyne, and J. B. Bremner. 2007. "In Vitro Cytotoxicity Evaluation of Some Substituted Isatin Derivatives." *Bioorganic & Medicinal Chemistry* 15 (2): 931–38. doi:10.1016/j.bmc.2006.10.035.

Wei, W.-B., S. Tian, H. Zhou, J. Sun, and H.-B. Wang. 2010. "5-Chloroindoline-2, 3-Dione." *Acta Crystallographica Section E Structure Reports Online* 66 (11): o3024. doi:10.1107/s1600536810042522.